

¹ **Estimating χ and K_T from fast-reponse thermistors on traditional shipboard**

² **CTDs: sources of uncertainty and bias.**

³ Andy Pickering*

⁴ *College of Earth, Ocean, and Atmospheric Sciences, Oregon State University, Corvallis, OR.*

⁵ Jonathan Nash

⁶ *College of Earth, Ocean, and Atmospheric Sciences, Oregon State University, Corvallis, OR.*

⁷ Jim Moum

⁸ *College of Earth, Ocean, and Atmospheric Sciences, Oregon State University, Corvallis, OR.*

⁹ Jen MacKinnon

¹⁰ *UCSD / Scripps Institute of Oceanography*

¹¹ *Corresponding author address: College of Earth, Ocean, and Atmospheric Sciences, Oregon State University, Corvallis, OR.

¹³ E-mail:

ABSTRACT

14 The acquisition of turbulence data from traditional shipboard CTD casts is
15 attractive for its potential to dramatically increase the amount of deep-ocean
16 mixing observations globally. While data from shear-probes are easily con-
17 taminated by motion of the instrument platform, the measurement of tempera-
18 ture gradient is relatively insensitive to vehicle vibration, making it possible to
19 measure temperature gradient from a shipboard CTD rosette. The purpose of
20 this note is to investigate and quantify the error and bias in estimating the rate
21 of dissipation of temperature variance χ and turbulent diffusivity K_T acquired
22 during traditional CTD profiling. The most significant source of error is as-
23 sociated with the fact that fast-response FP07 thermistors resolve only a frac-
24 tion of the temperature gradient variance at the fallspeed of typical CTD casts.
25 Assumptions must be made about the wavenumber extent of the temperature
26 gradient spectrum, which scales with the rate of dissipation of turbulent kinetic
27 energy, a quantity that is not directly measured. Here we utilize observations
28 from a microstructure profiler to demonstrate the validity of the method of es-
29 timating χ from thermistor data, and to assess uncertainty and bias. We then
30 apply this methodology to temperature gradient profiles obtained from χ pods
31 mounted on a CTD (the CTD- χ -pod), and compare these to microstructure
32 profiles obtained almost synoptically at the equator. CTD- χ -pod estimates of
33 χ compare favorably to the direct microstructure measurements and demon-
34 strate that the χ -pod method is not significantly biased. This supports the
35 utility of the measurement as part of the global repeat hydrography program
36 cruises, during which this type of data has been acquired during the past few
37 years.

³⁸ **1. Introduction**

³⁹ Turbulent mixing affects the distribution of heat, salt, and nutrients throughout the global ocean.

⁴⁰ Diapycnal mixing of cold, dense water with warmer water above maintains the abyssal overturning circulation (??), which affects global climate. ~~Due to sparse observations and the small scales at which mixing occurs, it is usually parameterized in climate models. Because the turbulence that drives mixing generally occurs at scales that are not resolved in climate models, it must be parameterized, based on either (i) aspects of the resolved model dynamics, (ii) through higher resolution models that capture the dynamics that feed energy to turbulence, or (iii) using other parameterizations that either dynamically or statistically quantify turbulent fluxes.~~ Recent investigations have demonstrated that these models are sensitive to the magnitude and distribution of mixing (?). ~~Better measurements are~~ A comprehensive set of measurements that spans relevant dynamical regimes is needed to constrain mixing and develop more accurate parameterizations.

⁵⁰ Direct measurement of mixing with microstructure profilers equipped with shear probes is expensive, time-intensive, and requires considerable care and expertise. Moreover, tethered profilers can't reach abyssal depths, requiring autonomous instruments to get deeper than \sim 1000-2000 m. As a result, existing measurements of diapycnal mixing, especially in the deep ocean, are sparse (?). In order to obtain estimates over a larger area, considerable work has gone into inferring mixing from ~~larger scales where measurements~~ measurements of the outer scales of turbulence, which are easier to obtain. One popular method is the use of Thorpe scales, where diapycnal mixing is inferred from inversions in profiles of temperature or density (??). The size of resolvable overturn is limited by the profiling speed and instrument noise (?). Several studies indicate relatively good agreement with microstructure and other observations, but there are some questions about the validity of the method and the assumptions made (??). Parameterizations based on profiles of shear

and/or strain have also been developed [and applied](#) to estimate diapycnal mixing (?????). However, they rely on a series of assumptions about the cascade of energy from large to small scales that are often violated; numerous studies (i.e., ?) have shown that there is significant uncertainty associated with [this method](#); [these parameterizations](#), in that there can be a consistent bias in a particular region, yet the sense of the bias (i.e., overpredict vs. underpredict) is not known [aprioria priori](#).

[Measurement of Quantifying](#) turbulence from velocity shear variance (to compute the dissipation rate of turbulent kinetic energy ε) is challenging on moorings or profiling platforms because there is usually too much vibration and/or package motion for shear-probes to be useful. Other methods (i.e., optics or acoustics) may hold some promise, but lack of scatterers often precludes this type of measurement, especially in the abyss. In addition, shear probes only provide ε , not the mixing of scalars, K , which is often inferred from ε by assuming a mixing efficiency $(?)\Gamma(?)$ as $K = \Gamma\varepsilon/N^2$, [which \$N^2\$ is the buoyancy frequency](#). A more direct measure of the turbulent mixing is obtained from the dissipation rate of temperature variance χ (?). This has the advantage that (i) temperature and temperature gradient [can be computed](#), [is relatively straightforawrd to measure](#), and (ii) the [estimation of mixing from \$\chi\$ does not rewuire assumptions about \$\Gamma\$](#) . However, the spectrum of temperature gradient extends to very small scales, so that its spectrum is seldom fully resolved (and unlike shear variance, the wavenumber extent of the spectrum is not related to the amplitude of the temperature (or temperature gradient) spectrum). Assumptions about the spectral shape (Kraichnan vs. Bachelor, and the value of the “constant” q) and its wavenumber extent (governed by the Batchelor wavenumber $k_b = [\varepsilon/(\nu D_T^2)]^{1/4}$ (?)) are thus necessary to determine χ unless measurements capture the full viscous-diffusive subrange of turbulence (i.e., down to scales $\Delta x \sim 1/k_b \sim 1\text{mm}$), a criterion seldom achieved. To resolve this, we follow [the assumptions of ?](#) and

? and make the assumption that $K_T = K_\rho$ to determine the dissipation rate as $\varepsilon_\chi = (N^2 \chi) / (2\Gamma < dT/dz >^2)$, permitting k_b to be estimated.

The goal of this paper is to outline and validate the methods used to compute χ and K_T with χ -pods mounted on CTDs. We do this by applying our processing [methods-methodology](#) to profile files of temperature gradient measured by thermistors on the ‘Chameleon’ microstructure profiler, which provides a direct test of our methodology. Because Chameleon is a loosely tethered profiler equipped with shear probes (Moum et al 1995), it directly measures ε and allows us to test our assumptions. Specifically, it allows us to determine biases associated with computing chi from partially-resolved temperature alone, as compared to that when it is computed by including knowledge of the dissipation rate, which constrains the wavenumber extent of the scalar spectra. After establishing that the method works, we then compare CTD- χ pod profiles to nearby microstructure profiles.

2. Data

a. EQ14

Data were collected on the R/V Oceanus in Fall 2014 during the EQ14 experiment to study equatorial mixing. More than 2700 Chameleon profiles were made, along with 35 CTD-chipod profiles bracketed by chameleon profiles in order to maintain calibrations during the cruise. Most Chameleon profiles were made to depth of about 250m, with CTD casts going to 500m or deeper. The EQ14 experiment and results are discussed in more detail in (Buoyant gravity currents released from tropical instability waves, JPO (SJ Warner, RN Holmes, EH McHugh-Hawkins, JN Moum) , in preparation).

105 **3. Methods**

106 As mentioned in the introduction, the temperature gradient spectrum is rarely fully resolved
107 down to the small scales of turbulent mixing. The ~~amount~~fraction of the spectrum resolved de-
108 pends on the true spectrum (a function of χ and ε), the flowspeed past the sensor ('fspd'), and
109 the response of the thermistor. The GE/Thermometrics FP07 thermistors we use typically resolve
110 frequencies up to about 10-15 Hz (??). The maximum resolved wavenumber is then equal to
111 $k_{max} = f_{max}/fspd$ ~~$k_{max} \equiv f_{max}/u$~~ , while the wavenumber extent of the true spectrum varies with
112 k_b (and the quarter power of ε). ~~At typical CTD fallspeeds of~~. At the typical vertical fall rate of a
113 CTD rosette ($\sim 1\text{m/s}$), only about 20% of k_b is resolved at $\varepsilon = 10^{-9}$ (Figure 2). ~~Methods that While~~
114 ~~methods~~ have been developed to fit the ~~temperature graident spectrum (?) work for much slower~~
115 ~~fallspeeds. However observed temperature gradient spectrum to theoretical forms (?)~~, these work
116 ~~only when a large fraction of the temperature gradient spectrum is resolved. For the relatively high~~
117 ~~profiling speeds typical of CTD casts~~, we find ~~that they these methods~~ do not work well ~~for higher~~
118 ~~speeds typical of CTD casts ($\approx 1\text{m/s}$) where much less of the spectrum is resolved~~ ((see appendix
119 for details) ~~+ and~~ therefore we use a different method.

120 We first outline our method for estimating χ , ~~and which relies on~~ (i) determining the
121 instantaneous flowspeed past the sensor, (ii) identifying periods where the signals may be
122 contaminated by the wake of the CTD rosette, (iii) defining the relavent N^2 and $(dT/dz)^2$, and
123 (iv) JN: WHAT ELSE?... We then discuss some limitations and practical considerations ~~that arise~~.

¹²⁴ a. Iterative Method for estimating χ

¹²⁵ For each ~ 1 second window, χ is estimated via the following procedure as outlined in ?. For
¹²⁶ isotropic turbulence,

$$\chi_T = 6D_T \int_0^\infty \Psi_{T_x}(k) dk \quad (1)$$

¹²⁷ where D_T is the thermal diffusivity and $\Psi_{T_x}(k)$ is the wavenumber spectrum of dT/dx .

¹²⁸ Note that dT/dx is not measured; dT/dt is measured, and dT/dx is inferred from Taylor's
¹²⁹ frozen flow hypothesis

$$\frac{dT}{dx} = \frac{1}{u} \frac{dT}{dt} \quad (2)$$

¹³⁰ The wavenumber extent of the spectrum depends on the ~~bateheler~~ Batchelor wavenumber k_b ,
¹³¹ which is related to ε :

$$k_b = [\varepsilon / (v D_T^2)]^{1/4} \quad (3)$$

¹³² We assume that ~~$K\rho = K_T$~~ $K_\rho = K_T$ and $K_\rho = \Gamma \varepsilon / N^2$. Then dissipation rate is computed as

$$\varepsilon_\chi = \frac{N^2 \chi_T}{2\Gamma \langle dT/dz \rangle^2} \quad (4)$$

¹³³ The Typical thermistors do not resolve the spectrum out to k_b ~~typically~~. So the measured portion
¹³⁴ of the, so the measured spectrum is fit to the Kraichnan form of theoretical scalar spectrum over the
¹³⁵ range of resolved wavenumbers ($k_{min} \leq k \leq k_{max}$). The variance between the measured $[\Phi_{T_x}(k)]_{obs}$
¹³⁶ and theoretical $[\Phi_{T_x}(k)]_{theory}$ spectra at ~~resolved~~ these wavenumbers is assumed to be equal:

$$\int_{k_{min}}^{k_{max}} [\Phi_{T_x}(k)]_{obs} dk = \int_{k_{min}}^{k_{max}} [\Phi_{T_x}(k)]_{theory} dk \quad (5)$$

¹³⁷ JN: need to explicitly state how χ is computed (integral of spectrum...).... ??? (you state a
¹³⁸ formula for ε_χ but not χ)

140 An iterative procedure is then used to fit and calculate χ and ε :

- 141 1. First we estimate χ_T based on an initial guess of $\varepsilon = 10^{-7}$ W/kg and compute k_b . We
142 set $k_{max} = k_b/2$ or to a wavenumber equivalent to $f_{max} = 7$ Hz [i.e., $k_{max} = 2\pi(f_{max})/u$],
143 whichever is smaller. We choose $f_{max} = 7$ Hz because the thermistors' response rolls off at
144 higher frequencies. ~~Measuring the transfer function for each individual thermistor proved~~
145 ~~too expensive and time-consuming. We found that using only frequencies up to 7Hz (where~~
146 ~~the transfer function is equal to or very close to unity) gives good agreement, and avoids the~~
147 ~~issue of the unknown transfer functions(see appendix).~~
- 148 2. We then use Eq. (4) to refine our estimate of k_b and recompute χ_T using Eqs. (1) and (5).
- 149 3. This sequence is repeated and converges after two or three iterations.

150 Note that this procedure is equivalent to the explicit formulation of (?), except we use the Kraich-
151 nan spectrum. JN and then it isn't possible to have the closed form the M used - us this true? If it
152 is, then state that, and if it isn't, then we should just solve for it..

153 b. CTD- χ -pod Data Processing

154 The basic outline for processing each CTD- χ -pod profile is as follows:

- 155 1. The correct time-offset for the χ -pod clock is determined by aligning dp/dt from the 24Hz
156 CTD data to vertical velocity calculated by integrating vertical accelerations measured by the
157 χ -pod. χ -pod clock drift is small, typically on the order of 1 sec/week, but it is imperative to
158 get records aligned within < 0.5 s so that the correct $u = w = dp/dt$ is used.
- 159 2. ~~The temperature and temperature derivative voltage signals from the Low-order polnomical~~
160 ~~calibration coefficients are determined to convert thermistor voltages from χ pod are~~

161 calibrated using a polynomial fit to CTD temperature to ITS90 temperature (as measured by
162 the CTD). Figure 3 shows an example of the aligned and calibrated CTD- χ pod timeseries for
163 one cast. Note that tempeature gradient signals are noiser on the downeast(upcast)for sensor
164 T1the significant differences in amount of variance associated with the two sensors during
165 down and up casts. For the upward-mounted sensor (T1), the downcast signal is entirely
166 associated with the CTD wake, as is the upcast for the downward-mounted sensor (T2), which
167 were mounted looking up and down, respectively. Only the ‘clean’ portion portions of the
168 cast (ie e.g., the T1 upcast)is and the T2 downcast) are used in the χ pod calculations.

169 3. Depth loops are identified and flagged in the 24Hz CTD data. χ -pod data during these times
170 are discarded since the signals are likely contaminated by the wake of the CTD. Even for
171 profiles that are significantly affected by ship heaving, good segments of data are obtained
172 over a majority of the depths.

173 4. Buoyancy frequency N^2 and temperature gradient dT/dz are compted from 1m-1-m binned
174 CTD data. *JN: I still like the idea of including some P data... but perhaps see below...*

175 5. Half-overlapping 1 sec windows of data are used to estimate χ , ε , and K_T following the
176 methods described in ?, outlined in the previous section. ~~The flow speed past the sensor is~~
177 ~~assumed to be equal to the fall speed of the package.~~

178 c. Example Spectra and Fits

179 An example of the observed and fit spectra are shown in Figure 4. Although only a small portion
180 of the spectrum is used in the fit, the method gives good results for χ . Errors in ε tend to be larger,
181 due to additional assumptions required.

182 JN: would be good to have a few more details, comment on the location, quick review of how
183 the spectrum is fit, etc. Also, maybe you could include the MLE estimate and MLE fit spectra to
184 show the differences?

185 JN: Perhaps you might also include 2 spectra? One for low and one for high epsilon?

186 *d. flowspeed past the sensor*

187 The flowspeed past the thermistor is needed to convert the measured temperature derivative
188 dT/dt to a spatial gradient. For the CTD- χ pod, the largest contribution to the flowspeed is usually
189 the vertical velocity of the CTD package (dp/dt), which is typically close to 1m/s –on average,
190 so we typically neglect the horizontal component of velocity in converting from frequency to
191 wavenumber spectra.

192 JN: but isn't it the swell-induced heave that is what sets the flow speed? I wonder if you
193 could/should show a series of spectra from some depth range over which chi/epsilon is relatively
194 constant, and then show a small snippet of data over which u changes appreciably, so that you
195 can see the different wavenumber spectra (maybe segregated by u (20-50 cm/s, 50-100 cm/s,
196 >100 cm/s)). I.e., you could show raw T, depth vs time, dT/dt , etc., so that you can see how
197 the data get contaminated, that you have to ignore the contaminated spectra, and then that the
198 non-contaminated parts are consistent, etc.

199 Although this will be a good approximation, errors may be introduced where horizontal veloci-
200 ties are large. Note that because b Because it is the total instantaneous velocity magnitude that is
201 used, represents flow past the sensor, neglecting the horizontal component of velocity (assuming
202 $u=dp/dt$ will always be a minimum estimate of) means we are always underestimating the true
203 flowspeed past the sensor. When the CTD package is equipped with LADCP, the true flowspeed
204 can be measured. In some cases (including EQ14) where the CTD was not equipped with LADCP,

205 it would seem that the ship's ADCP could be used to estimate the horizontal component of ve-
206 locity. However, because the CTD does not travel perfectly vertically in strong currents, this is
207 difficult to do in practice. In a strong horizontal flow, the CTD will drift with the current while de-
208 scending, lowering the flow relative to the sensors. On the upcasts, the CTD will be pulled against
209 the current, increasing the flow relative to the sensors. Since the CTD in EQ14 was not equipped
210 with LADCP, we use dp/dt as the flowspeed, and estimate potential errors in the appendix.

211 4. Oceanographic Setting and Conditions

212 Brief overview of dynamics in study region? More details are given in Warner et al (in prep).
213 JN - maybe you can omit this section, but add a few more details in section 2?

214 5. Results—~~Direct Test of χ_{pod} Method~~

215 a. Direct Test of χ_{pod} Method

216 We ~~first perform a test of our method of~~ begin by utilizing the highly-resolved turbulence profiler
217 ~~data (for which both ε and χ are measured)~~ to test the assumptions of equation in estimating χ by
218 applying 4 (e.g., how we compute n^2 , dt/dz , assumption of $\kappa_{\text{rho}} = k_t$, etc. We first apply) the χ_{pod}
219 method to each Chameleon profile, using only the FP07 thermistor data. These results, which we
220 will refer to as χ_{χ} , are ~~then~~ compared with χ_{ε} , computed by integrating the temperature gradient
221 spectrum with k_b computed directly from shear-probe derived ε . Qualitatively, χ_{χ} and χ_{ε} show
222 very similar depth and time patterns (Figure 5), suggesting the method generally works well. A
223 more quantitative comparison is made with a 2-D histogram (Figure 6), which shows that the two
224 are well-correlated over a wide range of magnitudes.

225 **6. Results - CTD χ -pod - Chameleon Comparison**

226 *a. CTD χ -pod - Chameleon Comparison*

227 Having demonstrated that the method works [for Chameleon data](#), we now compare χ from CTD-
228 mounted χ pods to χ_{ε} . In contrast to the [chameleon Chameleon](#) data, the CTD is more strongly
229 coupled to the ship, and therefore subject to more vibration, heaving, and artifical turbulence cre-
230 ated by the rosette. A total of 38 CTD- χ pod casts were done with chameleon profiles immediately
231 before and after. We first compare CTD- χ pod profiles to the mean of [chameleon Chameleon](#)
232 profiles bracketing each cast, both averaged in 5m depth bins (Figure 8). The two appear to be
233 correlated, with considerable scatter. However, we expect significant natural variability even be-
234 tween chameleon profiles. Scatter plots of before/after chameleon profiles (not shown), typically
235 separated by about an hour, show a similar level of scatter [as the differences between methods](#),
236 suggesting that the observed differences (Figure 8) can be explained by natural variability in tur-
237 bulence. This is demonstrated by histograms of the ratio of χ from adjacent casts (Figure 9) which
238 show that the variability between CTD χ pod and chameleon casts is similar to the natural vari-
239 ability between before/after chameleon profiles. Average profiles from all CTD-chameleon pairs
240 (Figure 10) overlap within 95% confidence limits at all depths where there exists good data for
241 both. Averages of subsets of profiles clustered in position/time (not shown) also agree.

242 **6. Discussion**

243 We have shown that χ can be accurately estimated from χ pods attached to CTD rosettes. [The](#)
244 [method also estimates \$c\$, but we have not discussed it here since it involves more assumptions and](#)
245 [uncertainties.](#)

246 *JN: I would consider going through each of the assumptions (maybe in bullets, to explain that*
247 *you test the effects of these (in the appendix, or elsewhere, and that they have small effect. include*
248 *gamma = 0.05, 0.1, 0.2, 0.4 and state explicitly the effect on χ . State the findings of n_2 , $dtdz$ too...?*

249

250 One major assumption is the mixing efficiency Γ . A value of 0.2 is commonly assumed, but
251 evidence suggests this may vary significantly. The χ_{pod} method also assumes that $K_T = K_\rho$. Even
252 if ε estimates have a large uncertainty, χ and K_T are robust and should be useful to the community.

253 *JN: Also make some summary statement of the amount of data thrown out because of swell*
254 *contamination, and make some statement about how you get the same answer regardless of*
255 *instantaneous dp/dt. For example, you could segregate data, and compute χ for all profiles,*
256 *including only instantaneous $u \leq 0.5$, and $u \geq 1.0$, and show that the 100-m means of those are*
257 *the same.... which means we're not getting contamination / bias from the variability in dp/dt?*

258 The goal of CTD- χ pods is to expand the number and spatial coverage of ocean mixing ob-
259 servations. We have already deployed instruments during several experiments (IWISE, TTIDE)
260 and on several GO-SHIP repeat-hydrography cruises. We plan to continue regular deployment on
261 GO-SHIP and similar cruises, adding χ and K_T to the suite of variables measured and enabling
262 scientists to explore relationships between these and other variables. The expanding database of
263 mixing measurements from CTD- χ pods will also enable testing of other commonly-used or new
264 mixing parameterizations. An example of data from a portion of the P16 GO-SHIP cruise is shown
265 in Figure 11.

266 **7. Conclusions**

267 Expand??

- The χ pod method was directly applied to temperature gradients measured by the chameleon microstructure profiler on 2742 profiles during the EQ14 cruises. The estimated χ_χ agrees well with χ_ε calculated using ε from shear probes over a wide range of magnitudes (Figure 6).
- CTD- χ pod profiles were also compared to nearby chameleon profiles during the cruise. Averaged profiles of χ agree within 95% confidence limits. No bias was detected between the estimates of χ .
- We conclude that estimates of χ and K_T from the CTD- χ pod platform are robust and reliable.

Acknowledgments. The EQ14 experiment was funded by ??. We thank the Captain and crew of R/V Oceanus. Also thank people who helped collect the data, those who made the sensors, etc..

APPENDIX A

Sensitivity to flowspeed

We investigate the sensitivity of the χ pod calculations to flowspeed, which is used to convert temperate gradient spectra from the frequency domain to the wavenumber domain via Taylor's frozen flow hypothesis. In this data, we have ignored any horizontal velocities and assumed the flow speed is equal to the vertical speed of the CTD rosette, determined from the recorded pressure dp/dt . To test the sensitivity of the χ pod method to flowspeed, we repeated the calculations with constant offsets added to the flowspeed. Since the total magnitude of velocity is used, dp/dt is a minimum estimate of the true speed. Adding 0.1(1)m/s results in a median error of 13(52) percent (Figure 12). Increasing the velocity tends to result in smaller values of χ , since it shifts the spectrum to lower wavenumbers.

APPENDIX B

Sensitivity to N^2 and dT/dz

291 We investigated the sensitivity of the calculations to N^2 , dT/dz . The iterative method to estimate
 292 chi requires the background stratification N^2 and temperature gradient dT/dz . We investigated the
 293 sensitivity of the results to the choice of scale over which these are computed or smoothed. The
 294 estimate of χ is insensitive to these scales. However, while dissipation rate ε and diffusivity K_T are
 295 more strongly affected because they are linearly related to these values. Computing N^2 and dT/dz
 296 over smaller scales results in larger values and hence some larger values of K_T .

APPENDIX C

Test of MLE fitting method

299 We tested the spectrum fitting method of ? and found that this method does not work well for
 300 the χ_{pod} data, where only a small fraction of the spectrum is resolved. In particular, the MLE
 301 method underestimates χ at larger magnitudes (Figure 13).

APPENDIX D

Variability of thermistor transfer functions

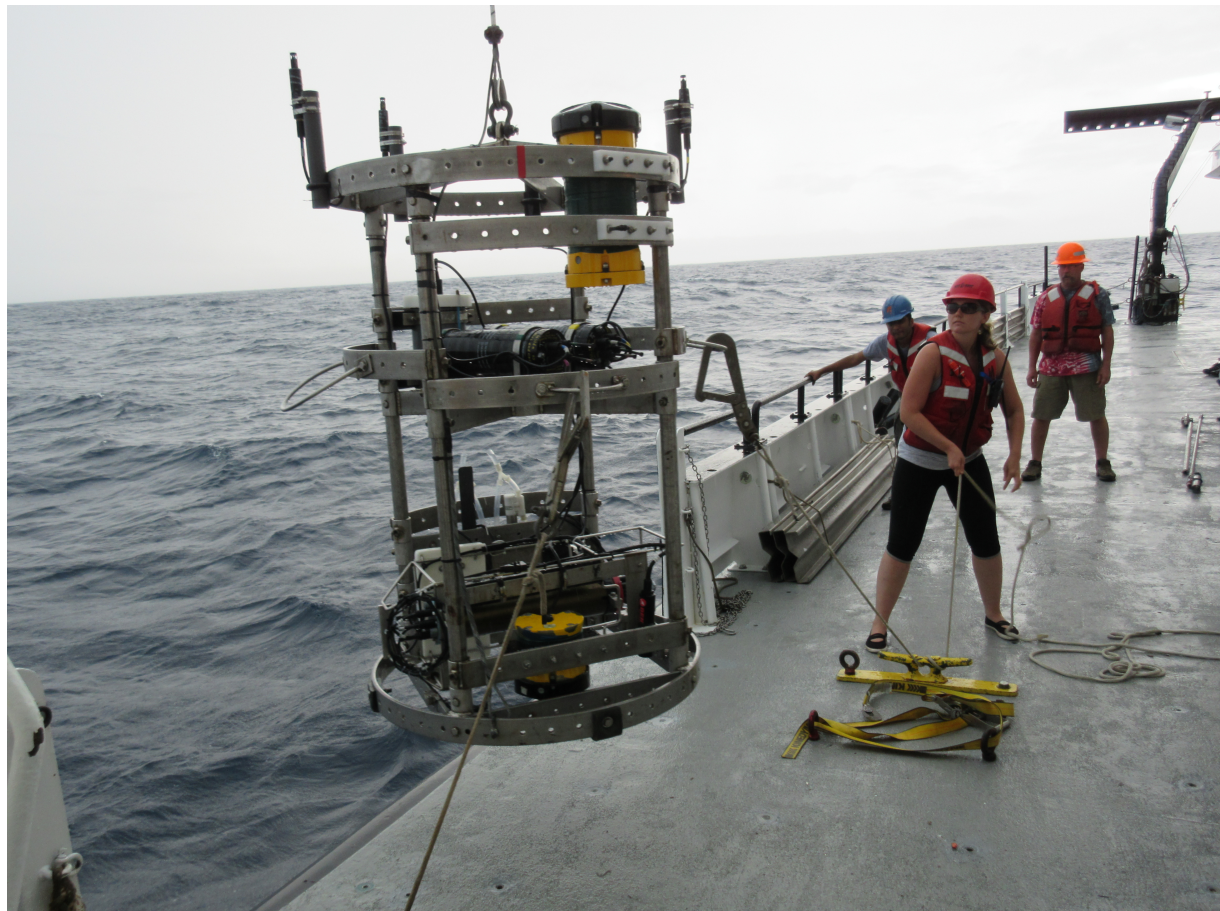
304 Measuring the transfer function for each individual thermistor proved too expensive and
 305 time-consuming. We found that using only frequencies up to 7Hz (where the transfer function
 306 is equal to or very close to unity) gives good agreement, and avoids the issue of the unknown
 307 transfer functions.

308 JN - I suggest you add the figure that shows the transfer functions for 10-20 thermistors, and has
309 a little histogram that convinces the reader that $XX = 90 \pm YY\%$ of the variance is resolved if one
310 chooses 7 Hz, but if you go out to 15-20 Hz, there is a large variability.

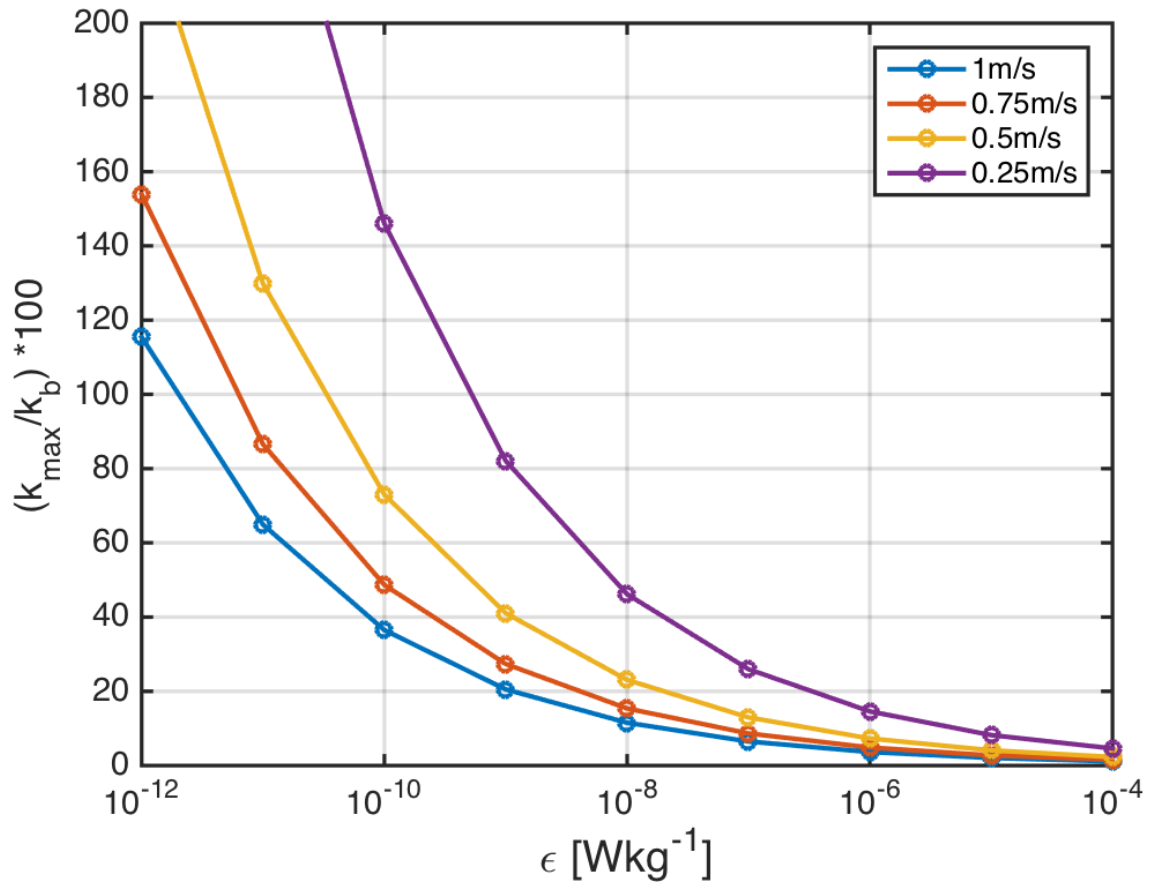
LIST OF FIGURES

311	Fig. 1.	Photo of CTD rosette during EQ14 with χ -pods attached. ** Add close-up picture of mini-chipod unit too**	20
312	Fig. 2.	Ratio of the maximum observed wavenumber $k_{max} = f_{max}/f_{spd}$ to the bachelor Batchelor wavenumber k_b for different values of ϵ , assuming a $f_{max} = 15\text{Hz}$. Each line is for a different flowspeed.	21
314	Fig. 3.	: add units / calibrate AX/AZ; also check to see if you've plotted dT/dt or $-dT/dt$. I think it has the wrong sign/ I think that's what comes out of the electronics; also label T1P and T2P series "up-looking dT_1/dt " and "down-looking dT_2/dt ". Example timeseries from one CTD cast during EQ14. a) CTD pressure. b) Fallspeed of CTD (dp/dt). c) Vertical and horizontal accelerations measured by χ -pod. d) Temperature from CTD and (calibrated) χ -pod sensors. T2 is offset slightly for visualization. e) Temperature derivative dT/dt measured by the upward-looking χ -pod sensor T1. f) Temperature derivative dT/dt measured by the downward-looking χ -pod sensor T2.	22
318	Fig. 4.	<i>JN: why choose an example where epsilon and epsilon chi are so different? Can we find a better one?</i> Example temperature gradient spectra from EQ14. Solid black line show the observed spectra. Dashed magenta line shows the fit theoretical Kraichnan spectra for the χ pod estimates. Purple line is Kraichnan spectra for chameleon χ and ϵ . Vertical dashed blue lines indicate the minimum and maximum wavenumber used in the χ pod calculation. The bachelor Batchelor wavenumber k_b is also indicated by the cyan line.	23
320	Fig. 5.	Depth-time plots of $\log_{10}\chi$ from both methods for EQ14 data. Top: χ pod method. Black diamonds indicate casts used for comparison with CTD- χ pod profiles. Bottom: Chameleon.	24
325	Fig. 6.	2D histogram of $\log_{10}(\chi)$ from chameleon (x-axis) and χ pod method (y-axes). Values from each profile were averaged in the same 5m depth bins.	25
326	Fig. 7.	Histogram of the (left) ratio of the maximum observed wavenumber k_{max} to the bachelor Batchelor wavenumber k_b , and (right) f_{spd} for all profiles in EQ14.	26
331	Fig. 8.	Scatter plot of χ from CTD- χ pod profiles versus the mean of bracketing chameleon profiles. Black dashed line shows 1:1, red are $\pm 10\chi$. **replace with histogram of ratios, or combine into one figure?**	27
332	Fig. 9.	Histogram of \log_{10} of the ratio of χ for nearby casts. The first set is for the before (cham1) and after (cham2) chameleon profiles. the 2nd is CTD- χ pod profiles versus the before(cham1) profiles. The last is CTD- χ pod profiles versus the after(cham2) profiles. Dashed lines show the medians of each set. Note that bias is small/zero, and the variability (spread) between CTD/cham is similar to the natural variability between cham profiles.	28
340	Fig. 10.	Time mean of χ for all CTD- χ pod - chameleon cast pairs, with 95% bootstrap confidence intervals.	29
347	Fig. 11.	Example chipod data from P16N. Top: $dTdz$. Bottom: χ	30
348	Fig. 12.	Histogram of % error for χ computed with constant added to fallspeed, in order to examine sensitivity to fallspeed.	31

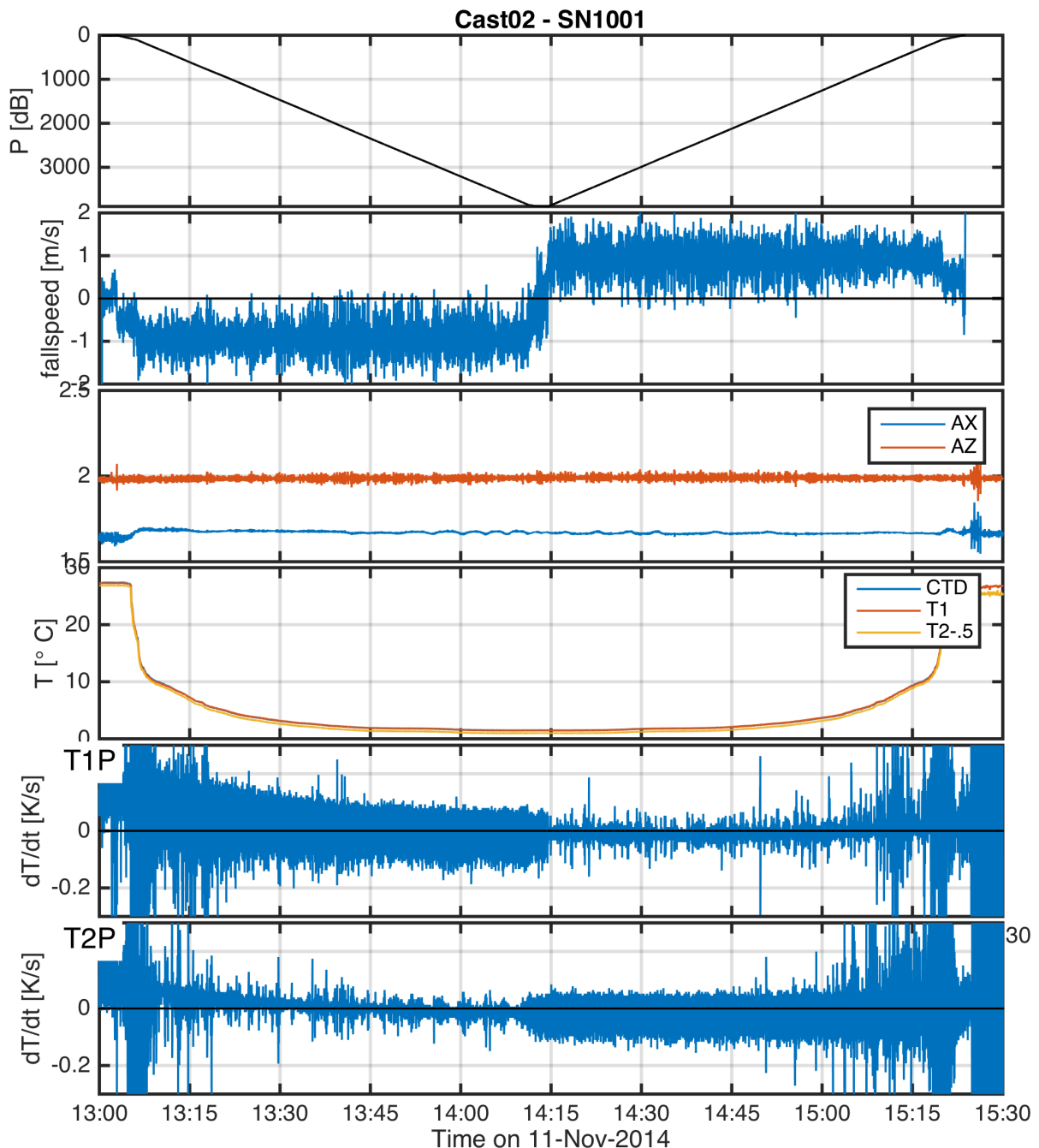
350 **Fig. 13.** 2D histograms of χ ~~from chipod~~ computed using the iterative χ -pod method (top; equation
351 XX) and ~~the~~ MLE fit (bottom; equation YY) fits versus ~~chameleon~~ χ computed from
352 Chameleon for EQ14 CTD-chipod casts. *JN - are you really using the CTD chipod casts and*
353 *not the Chameleon casts?* Note that the MLE method underestimates χ at larger magnitudes. . . 32



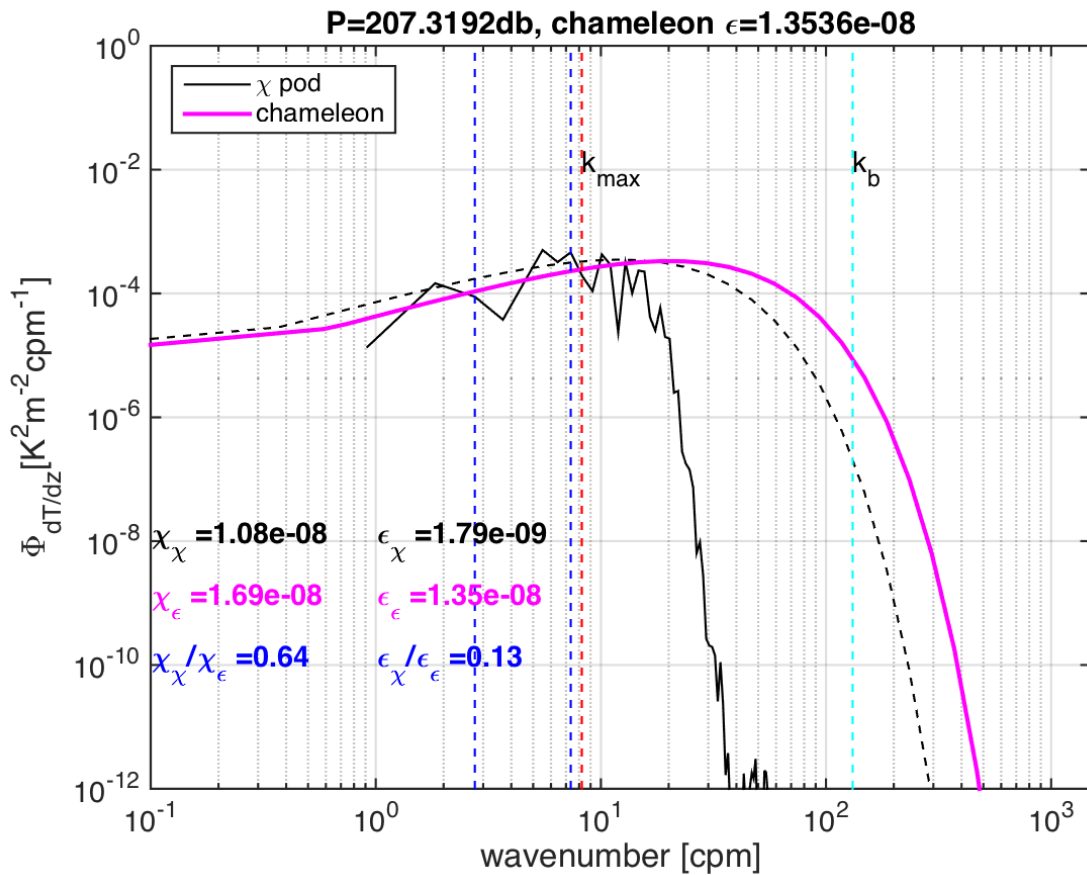
354 FIG. 1. Photo of CTD rosette during EQ14 with χ -pods attached. ** Add close-up picture of mini-chipod
355 unit too**



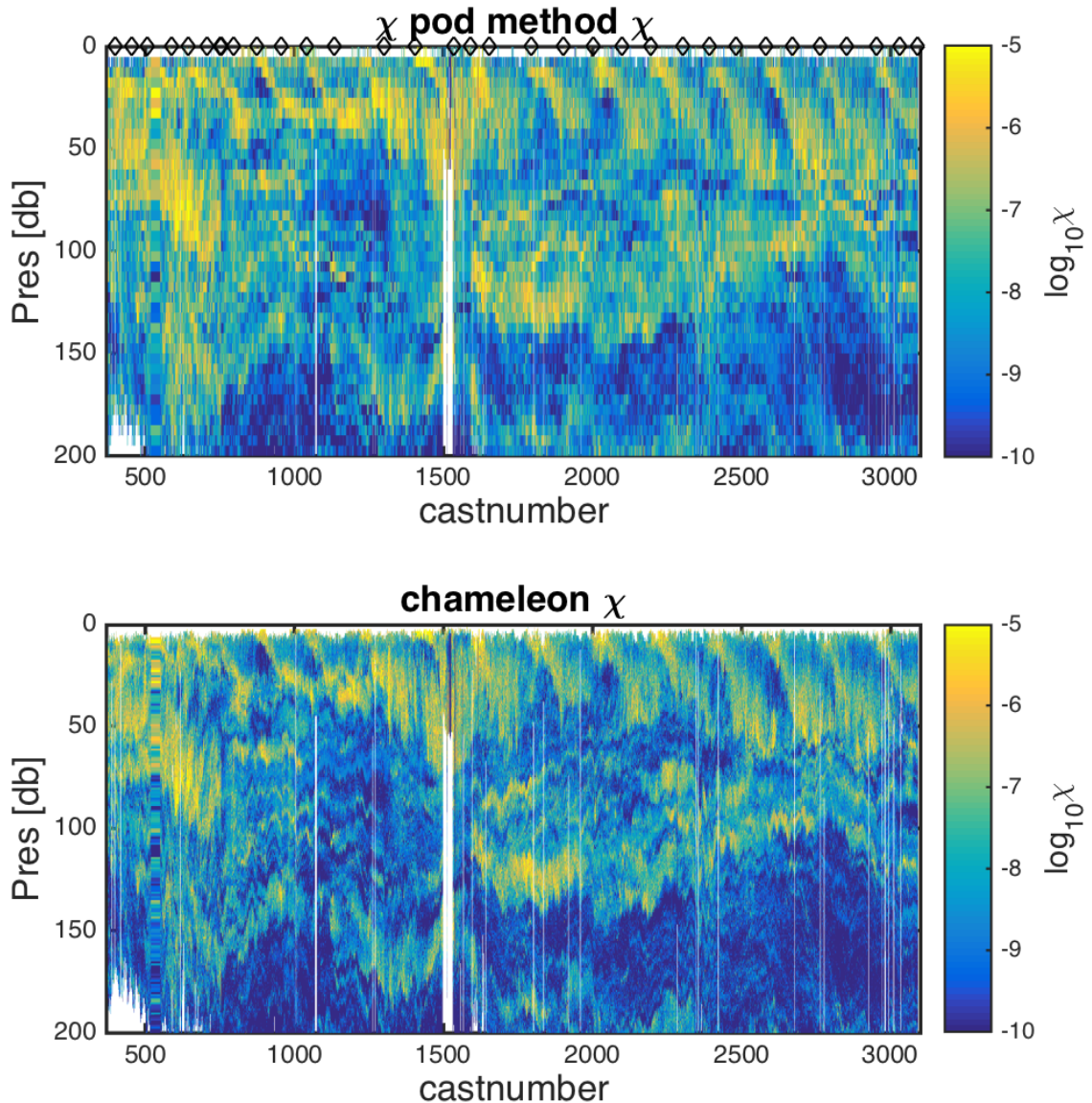
356 FIG. 2. Ratio of the maximum observed wavenumber $k_{max} = f_{max}/fspeed$ to the ~~bachelor~~ Bachelor wavenumber
 357 k_b for different values of ϵ , assuming a $f_{max} = 15Hz$. Each line is for a different flowspeed.



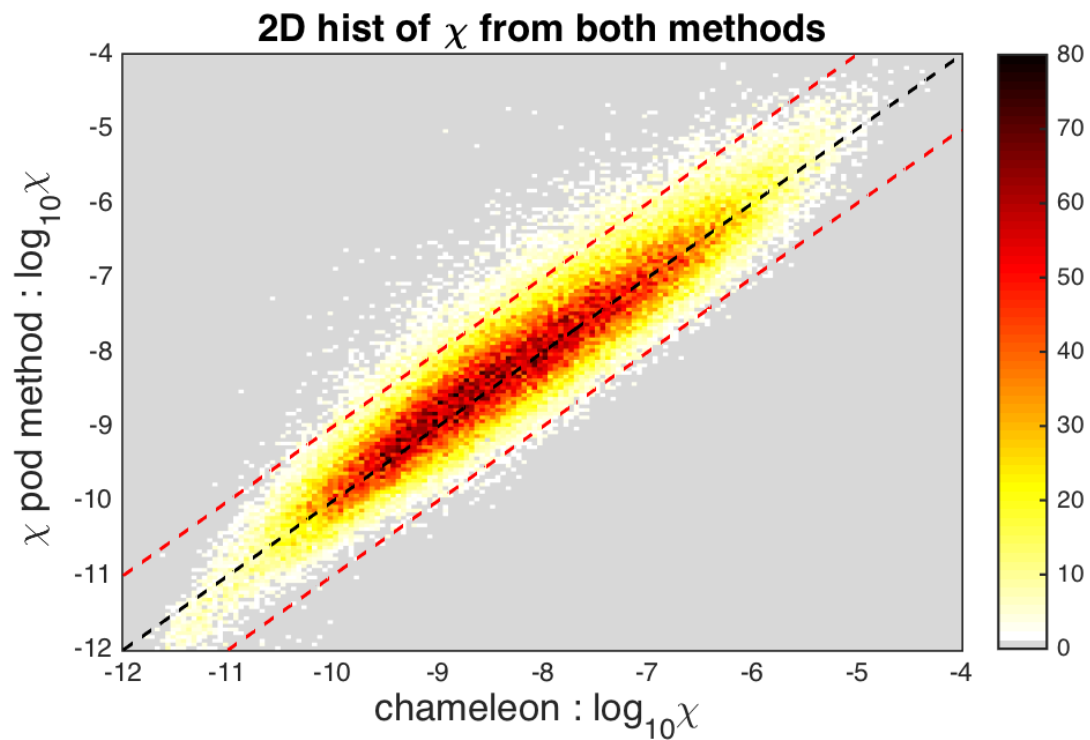
358 FIG. 3. : add units / calibrate AX/AZ; also check to see if you've plotted dT/dt or $-dT/dt$. I think it has the
 359 wrong sign/ I think that's what comes out of the electronics; also label T_1P and T_2P series "up-looking dT_1/dt "
 360 and "down-looking dT_2/dt ". Example timeseries from one CTD cast during EQ14. a) CTD pressure. b) Fallspeed
 361 of CTD (dp/dt). c) Vertical and horizontal accelerations measured by χ -pod. d) Temperature from CTD and
 362 (calibrated) χ -pod sensors. T_2 is offset slightly for visualization. e) Temperature derivative dT/dt measured
 363 by the upward-looking χ -pod sensor T_1 . f) Temperature derivative dT/dt measured by the downward-looking



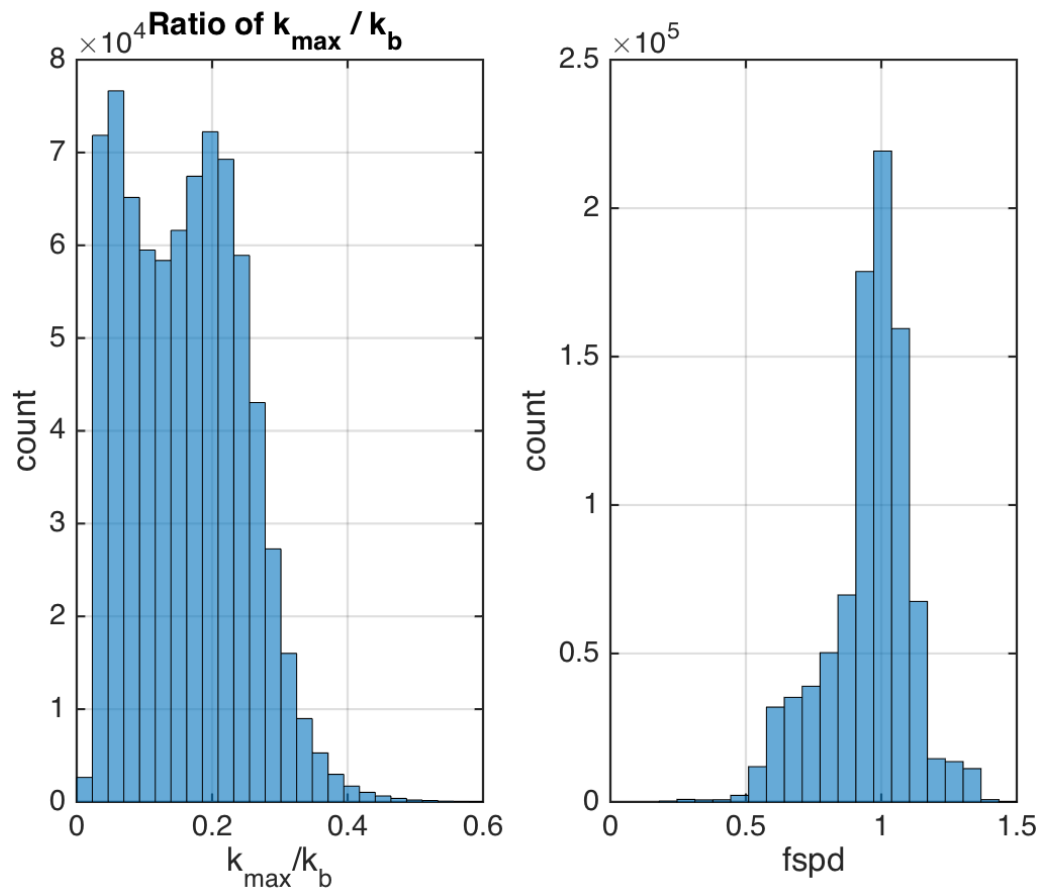
365 FIG. 4. JN: why choose an example where epsilon and epsilon chi are so different? Can we find a better
 366 one? Example temperature gradient spectra from EQ14. Solid black line show the observed spectra. Dashed
 367 magenta line shows the fit theoretical Kraichnan spectra for the χ pod estimates. Purple line is Kraichnan spectra
 368 for chameleon χ and ϵ . Vertical dashed blue lines indicate the minimum and maximum wavenumber used in the
 369 χ pod calculation. The batehelor Batchelor wavenumber k_b is also indicated by the cyan line.



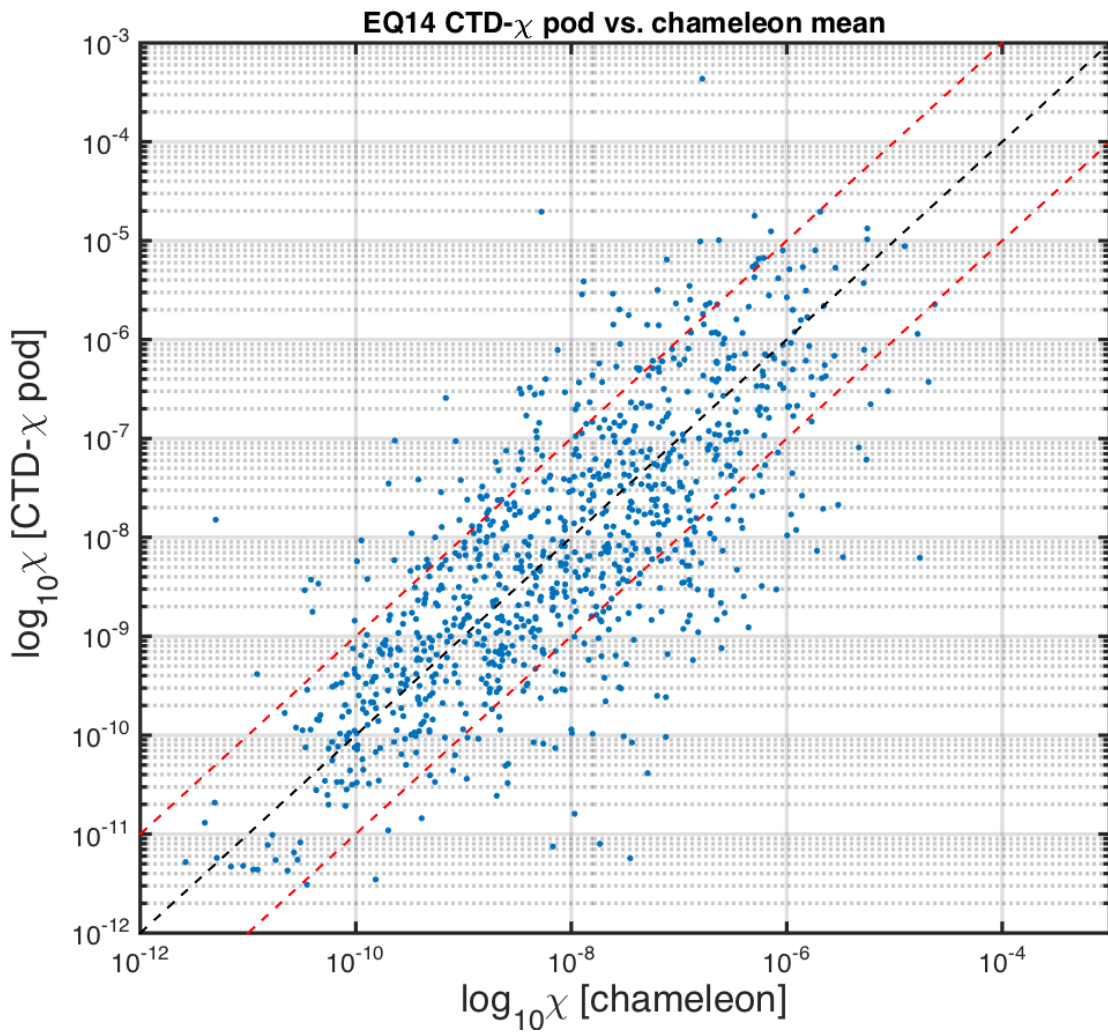
370 FIG. 5. Depth-time plots of $\log_{10} \chi$ from both methods for EQ14 data. Top: χ_{pod} method. Black diamonds
 371 indicate casts used for comparison with CTD- χ_{pod} profiles. Bottom: Chameleon.



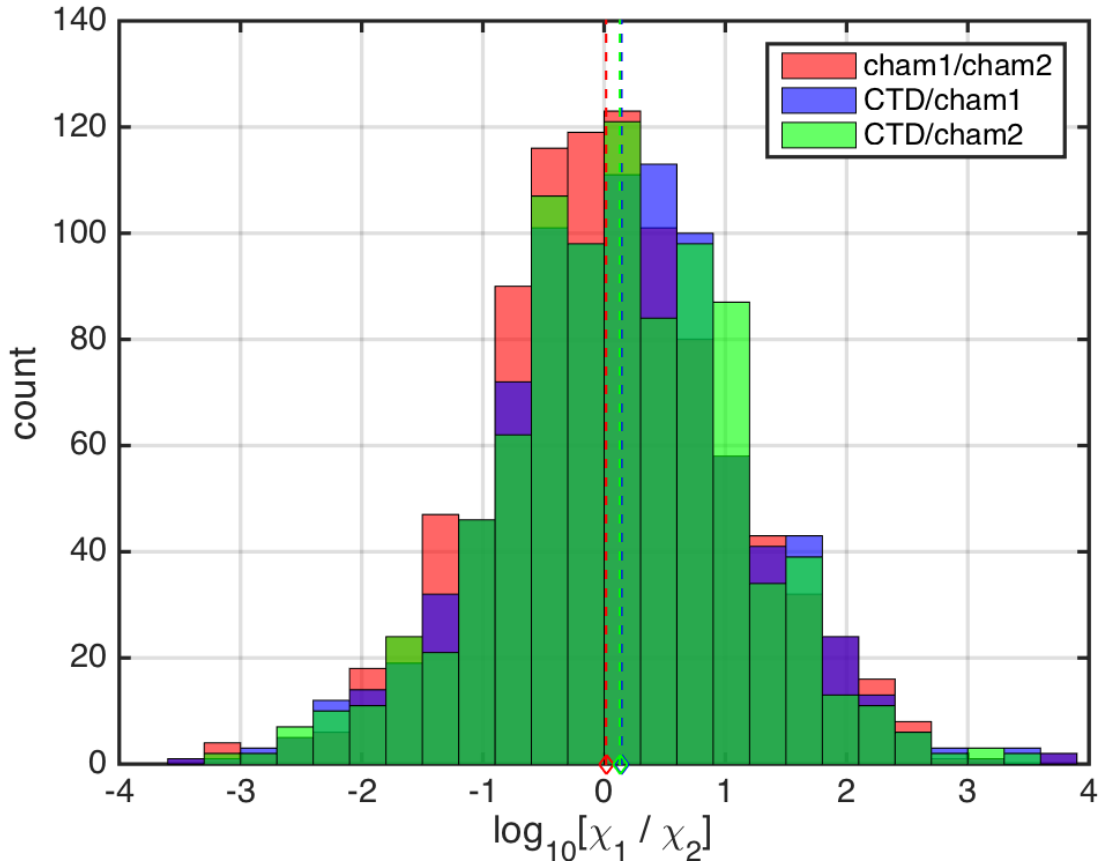
³⁷² FIG. 6. 2D histogram of $\log_{10}(\chi)$ from chameleon (x-axis) and χ_{pod} method (y-axes). Values from each
³⁷³ profile were averaged in the same 5m depth bins.



³⁷⁴ FIG. 7. Histogram of the (left) ratio of the maximum observed wavenumber k_{max} to the ~~bachelor~~ Batchelor
³⁷⁵ wavenumber k_b , and (right) fspd for all profiles in EQ14.



³⁷⁶ FIG. 8. Scatter plot of χ from CTD- χ pod profiles versus the mean of bracketing chameleon profiles. Black
³⁷⁷ dashed line shows 1:1, red are $\pm 10 \times$. **replace with histogram of ratios, or combine into one figure?**



378 FIG. 9. Histogram of \log_{10} of the ratio of χ for nearby casts. The first set is for the before (cham1) and
 379 after (cham2) chameleon profiles. the 2nd is CTD- χ pod profiles versus the before(cham1) profiles. The last is
 380 CTD- χ pod profiles versus the after(cham2) profiles. Dashed lines show the medians of each set. Note that bias
 381 is small/zero, and the variability (spread) between CTD/cham is similar to the natural variability between cham
 382 profiles.

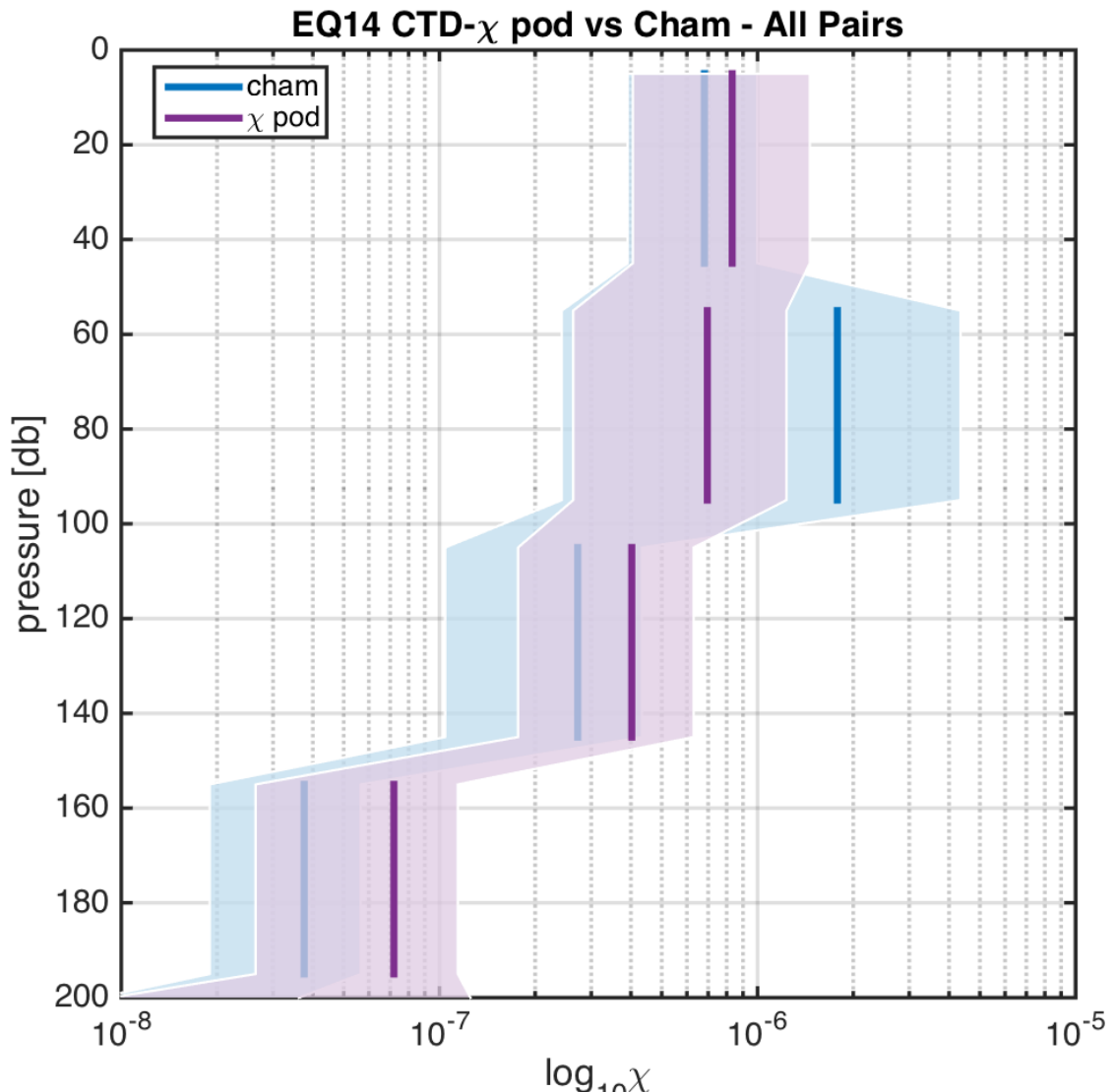


FIG. 10. Time mean of χ for all CTD- χ pod - chameleon cast pairs, with 95% bootstrap confidence intervals.

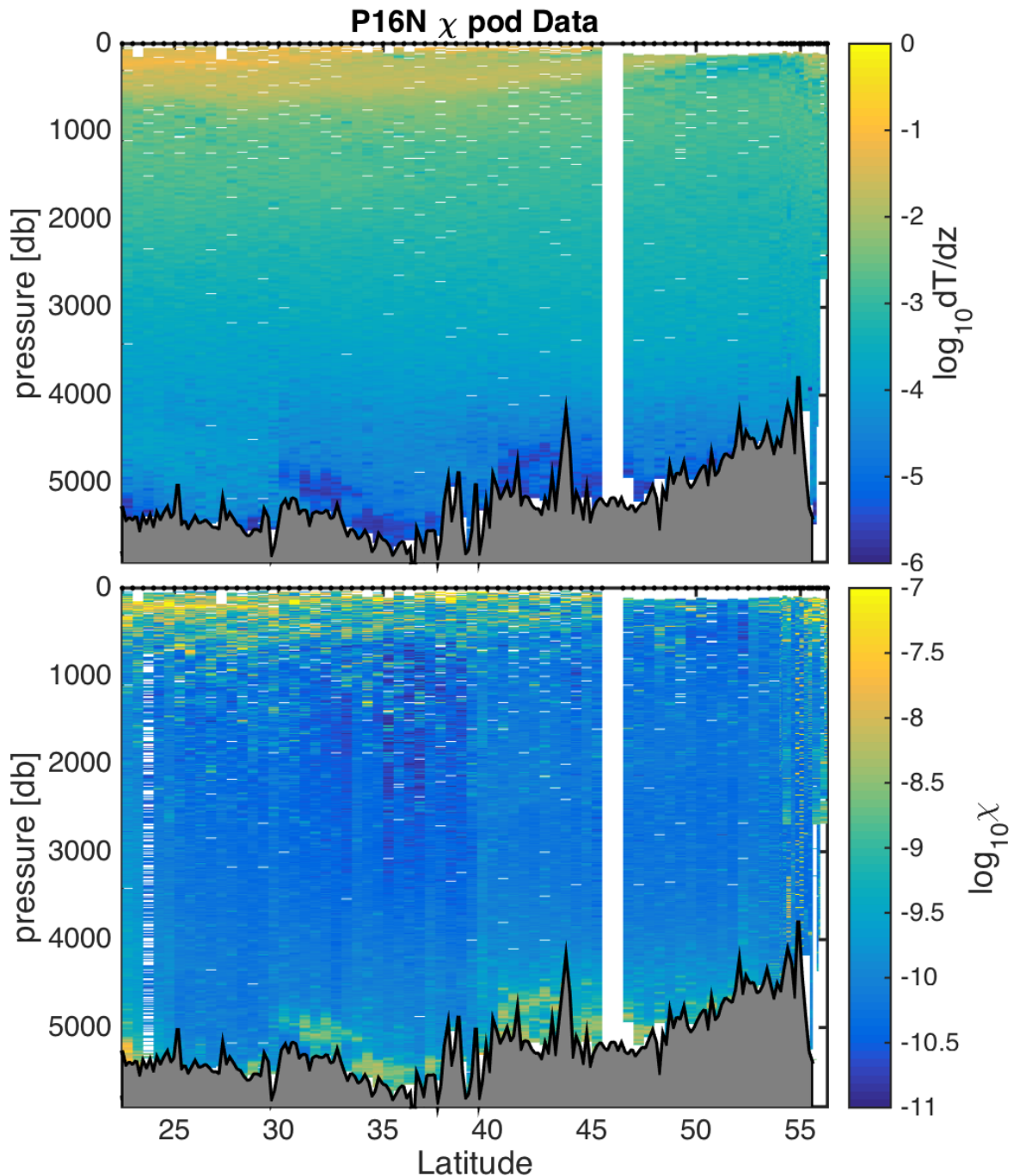
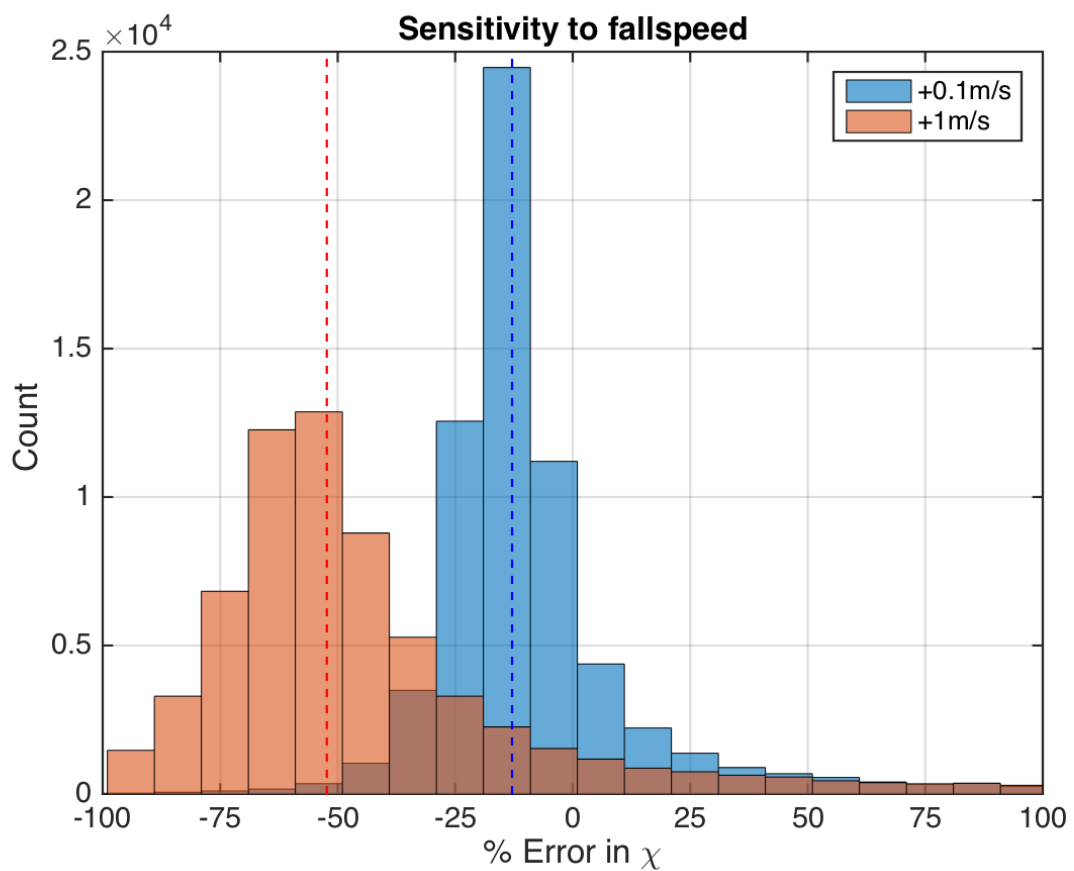
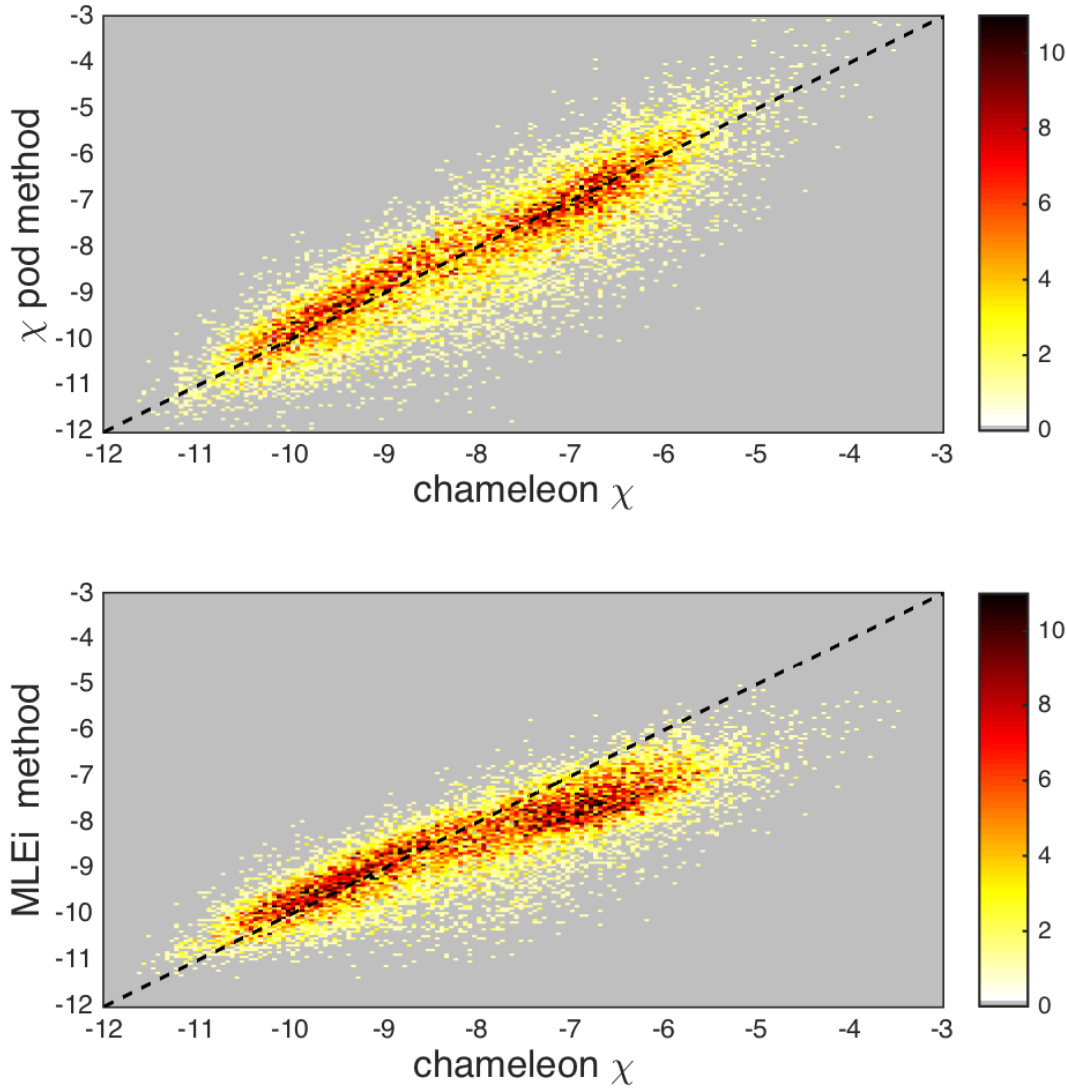


FIG. 11. Example chipod data from P16N. Top: $dTdz$. Bottom: χ .



383 FIG. 12. Histogram of % error for χ computed with constant added to fallspeed, in order to examine sensitivity
 384 to fallspeed.



385 FIG. 13. 2D histograms of χ [from chipod](#) computed using the iterative χ -pod method (top; [equation XX](#)) and
 386 [the MLE fit](#) (bottom; [equation YY](#)) [fits](#)-versus [chameleon](#)- χ computed from Chameleon [for EQ14 CTD-chipod](#)
 387 casts. [JN - are you really using the CTD chipod casts and not the Chameleon casts?](#) Note that the MLE method
 388 underestimates χ at larger magnitudes.